Journal of Molecular Liquids 311 (2020) 113286

Contents lists available at ScienceDirect

Journal of Molecular Liquids

journal homepage: www.elsevier.com/locate/molliq

Density, viscosity and free energy of activation for viscous flow of CO_2 loaded 2-amino-2-methyl-1-propanol (AMP), monoethanol amine (MEA) and H_2O mixtures

Sumudu S. Karunarathne, Dag A. Eimer, Lars E. Øi *

Faculty of Technology, Natural Sciences and Maritime Studies, University of South-Eastern Norway, Kjølnes Ring 56, Porsgrunn 3901, Norway

ARTICLE INFO

Article history:
Received 8 December 2019
Received in revised form 23 April 2020
Accepted 3 May 2020
Available online 13 May 2020

Keywords:
Density
Viscosity
2-Amino-2-methyl-1-propanol (AMP)
monoethanol amine (MEA)
Excess property

ABSTRACT

This work presents an experimental study of densities and viscosities of aqueous AMP (2-amino-2-methyl-1-propanol) + MEA (monoethanol amine) + H_2O solutions with and without CO_2. Amine concentrations were at AMP to MEA mass % ratios of 21/9, 24/6, 27/3 by maintaining 70 mass % of H_2O. Density measurements were performed in a temperature range from 293.15 K to 343.15 K and viscosity was measured at temperatures from 293.15 K to 363.15 K. The excess molar volume was determined from experimental density data. A Redlich-Kister type polynomial of excess molar volume was adopted to represent the density of unloaded aqueous mixtures. For CO_2 loaded solutions, Setschenow-type correlations and modified Weiland's density and viscosity correlations were used to fit density and viscosity data. Eyring's viscosity model was used to evaluate free energy of activation for viscous flow of mixtures through measured density and viscosity data. The volumetric and viscometric properties of aqueous mixtures were analyzed through the molecular structure and interactions. A correlation was proposed for the free energy of activation of viscous flow to represent viscosity of CO_2 loaded solutions. The results reveal that the proposed correlations for the density and viscosity of mixtures are in good agreement with measured data.

1. Introduction

The amine-based post combustion CO_2 capture (PCC) is regarded as a reliable and economical technology [1,2]. An absorbent having characteristics of higher capacity, faster absorption rates, lower heat of absorption and minimum hazardousness to the environment enables PCC more feasible for the industry [3]. Aqueous alkanolamines of monoethanol amine (MEA), methyldiethanolamine (MDEA) and diethanolamine (DEA) has been used in acid gas removal for decades. Conventional absorbents exhibit several disadvantages such as high regeneration energy, poor absorption capacity and amine degradation. As a result, the interest towards amine blends as an absorbent in CO_2 absorption has increased to optimize the energy demand and operational cost. The applicability of different amine blends have been tested to study mass transfer, reaction kinetics, solubility and absorption capacity [4–8] and pilot plant operations have been performed [9,10].

2-amino-2-methyl-1-propanol (AMP) is a sterically hindered primary amine and also known as the hinder form of MEA [8]. The attached two methyl group to the tertiary carbon atom in AMP hindered the formation of stable carbamate during the reaction with CO_2 [11]. Nwaoha, et al. [12] pointed that this increases the theoretical CO_2 absorption capacity up to 1 mol CO_2/mol amine. The molecular structure of AMP is illustrated in Fig. 1. MEA is the benchmark absorbent in amine-based PCC to compare the other absorbent for the characteristics of absorption rate, absorption capacity and degradation. Although MEA has a high absorption rate, it has limited thermodynamic capacity to absorb CO_2 [11]. An aqueous blend of AMP and MEA could overcome the drawbacks of individual aqueous solutions. Mandal and Bandyopadhyay [13] emphasized that increase of MEA in an aqueous AMP solution increased the enhancement factor and rate of absorption over single amine aqueous MEA and AMP mixtures. Another study performed by Sakwattanapong, et al. [5] revealed an increase of overall rate constant in AMP + MEA + H_2O mixtures with MEA concentration. These observations conclude that the mixture of AMP + MEA + H_2O is a potential alternative for CO_2 absorption.

In order to investigate the performance of these blends in pilot or large scale, further studies are required in the form of mathematical modelling and simulations of the absorption and desorption process. In that, available data of measured physical properties like density and viscosity in both CO_2 loaded and unloaded aqueous amine blend is a key factor to perform accurate

* Corresponding author.
E-mail addresses: sumudu.karunarathne@usn.no (S.S. Karunarathne), dag.a.eimer@usn.no (D.A. Eimer), lars.oi@usn.no (L.E. Øi).

https://doi.org/10.1016/j.molliq.2020.113286

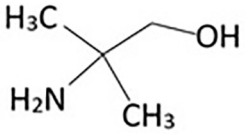

IUPAC name: 2-amino-2-methyl-propan-1-ol

Fig. 1. Molecular structure of AMP.

simulations and engineering design calculations. Measured data of density and viscosity of AMP + MEA + H_2O mixtures are reported in the literature [14,15].

In this study, the focus was given to measure density and viscosity of both aqueous and CO_2 loaded mixtures of AMP + MEA + H_2O under different amine mass ratios, CO_2 loadings and temperatures at a pressure of 4 bar (N_2 gas). The excess molar volumes were determined for the AMP + MEA + H_2O liquid mixtures and correlated by a Redlich-Kister [16] type polynomial. Same correlation was used to correlate the density of aqueous mixtures and was compared with measured data. For the mixtures of AMP + MEA + H_2O + CO_2, a Setschenow-type correlation and a modified Weiland's density correlation [17] were considered to correlate the densities. For the viscosities, a Setschenow-type correlation and a modified Weiland's viscosity correlation were adopted for the data fit.

The reported density and viscosity of aqueous solutions from Mandal, et al. [14] were considered to find the excess free energy of activation for viscous flow ΔG^{E*} according to the absolute rate theory approach of Eyring [18] on dynamic viscosity of a Newtonian fluid. A correlation based on a Redlich-Kister polynomial was suggested to correlate ΔG^{E*} and examine the possibilities to represent the unloaded solution viscosities. The viscosity deviations η^E were determined to examine the types of interaction between component molecules in the mixtures. The free energy of activation for viscous flow ΔG^* was determined by adopting Eyring's dynamic viscosity model. The difference of ΔG^* between CO_2 loaded and aqueous AMP + MEA + H_2O mixtures was considered to correlate ΔG^* of CO_2 loaded solutions. Finally, the proposed correlation was examined for the representation of measured viscosity of CO_2 loaded solutions.

2. Experiments

A description of materials that are used for the all experiments are listed in Table 1. Deionized water (Milli-Q water/resistivity 18.2 MΩ·cm) and chemicals were degassed by using a rotary evaporator (BUCHI, Rotavapor R-210) before the solution preparation. Aqueous solutions of AMP + MEA were prepared on the mass basis (analytical balance Mettler Toledo XS-403S with an accuracy of ± $1 \cdot 10^{-7}$ kg).

Carbon dioxide was added to the aqueous amine blend by bubbling it through the mixture until the solution was saturated. The solution pH was measured (Mettler Toledo InLab pt. 1000) during the CO_2 loading and CO_2 supply was stopped when the pH became steady around pH = 8. The CO_2 loading was performed under atmospheric pressure at room temperature. Then the CO_2 loaded sample was stored in a refrigerator for 24 h to complete the reactions before it was used to prepare a series of CO_2 loaded aqueous amine mixtures by mixing with CO_2 unloaded aqueous amine mixtures. All the CO_2 loaded and CO_2 unloaded aqueous amine mixtures were stored in a refrigerator until they were used in density and viscosity measurements.

The CO_2 concentration in all prepared mixtures was determined by a method based on precipitation of $BaCO_3$ and titration [19,20]. A sample of (0.25–0.3) g was mixed with 50 mL of 0.1 mol·L^{-1} NaOH and 0.3 mol·L^{-1} $BaCl_2$. Then the mixture was boiled for 10 min (approximately) in order to complete the precipitation reaction and was cooled in a water bath. The precipitate was filtered through a hydrophilic polypropylene membrane filter (45 μm). The filter cake was transferred into 100 mL of deionized water and was titrated with 0.1 mol·L^{-1} HCl until the solution pH reached a value 2. Then the excess HCl was determined by titrating back with 0.1 mol·L^{-1} NaOH solution. Finally, the amine concentration was analyzed through a separate titration in which a sample of 1 g was transferred into 100 mL of deionized water and titrated with 1 mol·L^{-1} HCl.

Table 1
Materials used in this study.

Chemical name	CAS reg. no.	Source	Purity
2-Amino-2-methyl-1-propanol (AMP)	124-68-5	Sigma-Aldrich	BioUltra, ≥99.0% (GC)[a]
Monoethanol amine (MEA)	141-43-5	Sigma-Aldrich	≥99.5% (GC)[a]
Carbon dioxide (CO_2)	124-38-9	AGA Norge AS	≥99.9%
Nitrogen (N_2)	7727-37-9	AGA Norge AS	≥99.9%
Sodium hydroxide (NaOH)	1310-73-2	Merck KGaA	–
Hydrochloric acid (HCl)	7647-01-0	Merck KGaA	–
Barium chloride dehydrate ($BaCl_2 \cdot 2H_2O$)	10326-27-9	Merck KGaA	≥99.0%

[a] Gas chromatography.

Table 2
Experimental data of the density ρ/kg·m^{-3} of pure AMP from this work and literature data at different temperatures.

T/K	ρ/kg·m^{-3}				
	This work	Literature			
		Aguila-Hernández, et al. [24]	Henni, et al. [25]	Xu, et al. [26]	Zhang, et al. [27]
303.15					925.72
308.15	921.4				921.48
313.15	917.3	917.2	919.65	921.1	917.30
318.15	913.3				913.09
323.15	909.1	909.2	911.24	913.4	908.86
328.15	905.0				904.59
333.15	900.4	900.7	902.87	905.5	900.29
338.15	896.0				895.95
343.15	891.6		894.28		891.57
348.15	887.2				887.18
353.15	882.7				882.75
358.15	878.3				
363.15	873.7				

2.1. Density measurement

Density measurements were performed using an Anton Paar DMA 4500 density meter. A sample of 3–5 mL volume (typically

Table 3
Experimental data of the density ρ/kg·m^{-3} and excess molar volume V^E/m^3·mol^{-1} of AMP (1) + MEA (2) + H_2O (3) at different amine mass (%) and temperatures.

Mixtures	AMP (mass %)/MEA (mass %)					
	21/9		24/6		27/3	
T/K	ρ	$10^6 \cdot V^E$	ρ	$10^6 \cdot V^E$	ρ	$10^6 \cdot V^E$
293.15	1003.5	−0.4216	1002.2	−0.4530	1000.8	−0.4836
298.15	1001.1	−0.4193	999.7	−0.4504	998.2	−0.4786
303.15	998.5	−0.4167	997.1	−0.4461	995.6	−0.4743
308.15	995.8	−0.4133	994.3	−0.4417	992.7	−0.4689
313.15	993.0	−0.4097	991.4	−0.4369	989.7	−0.4629
318.15	990.0	−0.4054	988.3	−0.4322	986.7	−0.4574
323.15	986.9	−0.4021	985.3	−0.4288	983.5	−0.4517
328.15	983.7	−0.3985	982.0	−0.4236	980.2	−0.4467
333.15	980.4	−0.3949	978.6	−0.4197	976.8	−0.4417
338.15	976.9	−0.3906	975.1	−0.4146	973.3	−0.4372
343.15	973.4	−0.3876	971.6	−0.4121	969.7	−0.4329

Table 4
Binary parameters A_0, A_1 and A_2 of the equation $V^E_{jk} = x_j x_k \sum_{i=0}^{n} A_i (x_j - x_k)^i$ for the excess molar volume for AMP (1) + MEA (2) + H_2O (3).

Parameters		Binary pair		
		AMP + MEA	MEA + H_2O	AMP + H_2O
A_0	$a/(m^3 \cdot mol^{-1})$	−1066.4 ± 0.5	−406.99 ± 0.02	177.15 ± 0.02
	$b/(m^3 mol^{-1} \cdot K^{-1})$	−0.1621 ± 0.001	0.14392 ± 0.00006	$0.72728 \pm 6 \cdot 10^{-5}$
	$c/(m^3 \cdot mol^{-1} \cdot K^{-2})$	−3.130114 ± 0.000005	$0.6862104 \pm 4 \cdot 10^{-7}$	$0.5239493 \pm 2 \cdot 10^{-7}$
A_1	$a/(m^3 \cdot mol^{-1})$	600,519 ± 15	412.87 ± 0.04	−203.460 ± 0.015
	$b/(m^3 \cdot mol^{-1} \cdot K^{-1})$	89.01 ± 0.08	0.6387 ± 0.0001	$1.11910 \pm 6 \cdot 10^{-5}$
	$c/(m^3 \cdot mol^{-1} \cdot K^{-2})$	31.5940 ± 0.0003	$1.1123489 \pm 4 \cdot 10^{-7}$	$1.0886053 \pm 3 \cdot 10^{-7}$
A_2	$a/(m^3 \cdot mol^{-1})$	−17,479,306 ± 450	−415.370 ± 0.035	237.27 ± 0.03
	$b/(m^3 \cdot mol^{-1} \cdot K^{-1})$	−2284 ± 3	0.2524 ± 0.0004	$0.4501 \pm 1 \cdot 10^{-4}$
	$c/(m^3 \cdot mol^{-1} \cdot K^{-2})$	−301.819 ± 0.008	$0.5735243 \pm 4 \cdot 10^{-7}$	$0.5617385 \pm 4 \cdot 10^{-7}$

holds about 0.7 mL of sample) was introduced into the oscillating U tube that is oscillated at its fundamental frequency. The instrument is capable of measuring density with ±0.05 $kg \cdot m^{-3}$ accuracy and can be operated in a temperature range of 273.15 K to 363.15 K (± 0.03 K) under atmospheric condition. A density check was performed to check the validity of the factory adjustment. A standard density reference S3S from Paragon Scientific Ltd. was used to record any possible deviations in the measurements. Density measurements of both aqueous amine blends and CO_2 loaded aqueous amine blends were done under atmospheric condition for the temperature range of 293.15 K–343.15 K. In order to minimize the error due to evaporation of amines and CO_2, a new sample was fed into the density meter at each temperature level.

2.2. Viscosity measurements

The dynamic viscosity of all solutions was measured using a Physica MCR 101 rheometer with a double-gap pressure cell XL from Anton Paar. A sample of 7 mL was placed using a clean syringe into the volume occupied between two cylinders. The temperatures >303.15 K was controlled by an internal temperature controlling system with a temperature accuracy of ±0.03 K while an external cooling system of Anton Paar Viscotherm VT2 with temperature accuracy of ±0.02 K was adopted to control temperatures below 303.15 K. Calibration of the instrument was done using a viscosity reference standard S3S from Paragon Scientific Ltd. The viscosity deviations were recorded by comparing measured viscosity of a standard solution with the reference viscosities at temperatures specified by the supplier. Accordingly, experimental observations have been corrected for those deviations. An expected deviation was considered by interpolation at the temperatures where the standard reference viscosities have not been provided by the manufacturer. As a preventive measure for the possible degassing of CO_2 from mixtures at higher temperatures, the viscosity measurements were performed at 4 bar nitrogen atmosphere in the temperature range of 293.15 K–363.15 K. As per our knowledge, the composition variation of mixtures before and after the experiments is negligible [21] and the effect of pressure on viscosity was in the order of 0.01%.

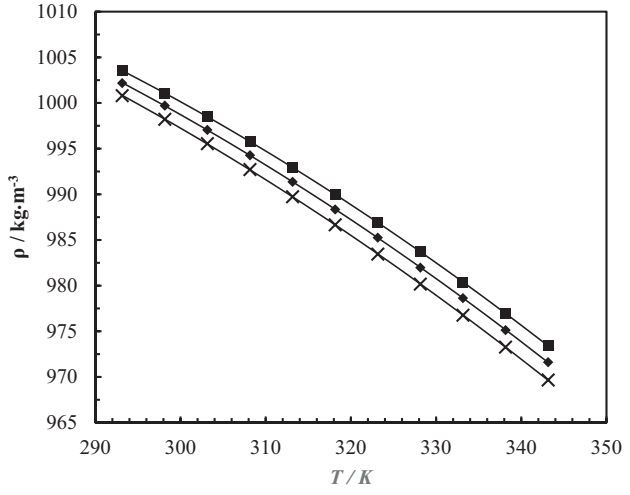

Fig. 2. Density of AMP + MEA + H_2O mixtures: measured data; 21 mass % AMP + 9 mass % MEA + 70 mass % H_2O, '■', 24 mass % AMP + 6 mass % MEA + 70 mass % H_2O, '◆', 27 mass % AMP + 3 mass % MEA + 70 mass % H_2O, 'x', correlation from Eq. (3) to Eq. (6); '———'.

3. Experimental Uncertainty

The combined standard uncertainty of density and viscosity measurements of aqueous amine mixtures was determined by considering several uncertainty sources of material purity $u(p)$, temperature measurement$u(T)$, calibration $u(c)$, weight measurement $u(w)$, CO_2 loading $u(\alpha)$ and repeatability $u(rep)$.

In the uncertainty of density measurement, considered standard uncertainties were $u(p) = \pm 0.006$, $u(T) = \pm 0.012$ K, $u(c) = 0.01 kg \cdot m^{-3}$, $u(w) = \pm 2 \times 10^{-4}$ kg, $u(\alpha) = \pm 0.005$ mol CO_2/mol amine and $u(rep) = \pm 0.13\ kg \cdot m^{-3}$. The maximum gradient of density against temperature, $\partial\rho/\partial T$, was found as $0.9\ kg \cdot m^{-3} \cdot K^{-1}$ and the corresponding uncertainty in ρ, $(\partial\rho/\partial T) \cdot u(T)$ was calculated as $\pm 0.011\ kg \cdot m^{-3}$. The gradient of density against CO_2 loading, $\partial\rho/\partial\alpha$, was found as $236\ kg \cdot m^{-3}$ and the corresponding uncertainty in ρ, $(\partial\rho/\partial\alpha) \cdot u(\alpha)$ was determined as $\pm 1.18\ kg \cdot m^{-3}$. The Guide to the Expression of Uncertainty in Measurement [22,23] was followed to evaluate combined standard uncertainty for the density measurement by considering all mentioned uncertainty sources as $u(\rho) = \pm 6.63\ kg \cdot m^{-3}$. Then the combined expanded uncertainty of the density measurement $U(\rho)$ was found as $= \pm 13.3\ kg \cdot m^{-3}$ (level of confidence = 0.95).

In the uncertainty of viscosity measurement, considered standard uncertainties for the uncertainty sources are $u(p) = \pm$

Table 5
Density $\rho/kg \cdot m^{-3}$ of CO_2 loaded 21 mass % AMP + 9 mass % MEA + 70 mass % H_2O at different temperatures and CO_2 loadings (α/mol CO_2·mol amine^{-1}).

$\alpha/(mol\ CO_2 \cdot mol\ amine^{-1})$	0.107	0.210	0.308	0.400	0.518
x_4	0.0095	0.0185	0.0269	0.0346	0.0444
T/K	$\rho/kg \cdot m^{-3}$				
293.15	1019.8	1036.4	1053.6	1071.3	1087.2
298.15	1017.4	1034.0	1051.1	1068.7	1084.5
303.15	1014.9	1031.5	1048.6	1066.0	1081.7
308.15	1012.2	1028.9	1045.9	1063.2	1078.9
313.15	1009.4	1026.1	1043.2	1060.3	1075.9
318.15	1006.6	1023.3	1040.3	1057.3	1072.9
323.15	1003.6	1020.3	1037.4	1054.4	1070.0
328.15	1000.5	1017.3	1034.3	1051.3	1066.7
333.15	997.2	1014.2	1031.2	1048.0	1063.4
338.15	993.8	1011.0	1027.9	1044.7	1059.4
343.15	990.4	1007.5	1024.6	1041.3	1054.9

Table 6
Density ρ/kg·m^{-3} of CO_2 loaded 24 mass % AMP + 6 mass % MEA + 70 mass % H_2O at different temperatures and CO_2 loadings (α/mol CO_2·mol amine^{-1}).

α/(mol CO_2·mol amine^{-1})	0.083	0.165	0.314	0.418	0.508
x_4	0.0071	0.0141	0.0264	0.0349	0.0420
T/K	ρ/kg·m^{-3}				
293.15	1014.8	1029.4	1049.4	1066.4	1081.6
298.15	1012.3	1026.9	1046.8	1063.5	1078.6
303.15	1009.7	1024.3	1044.1	1060.5	1075.5
308.15	1006.9	1021.6	1041.2	1057.4	1072.3
313.15	1004.1	1018.8	1038.2	1054.3	1069.0
318.15	1001.1	1015.8	1035.2	1051.0	1065.7
323.15	998.0	1012.8	1032.0	1047.7	1062.3
328.15	994.8	1009.6	1028.8	1044.3	1058.9
333.15	991.5	1006.4	1025.5	1040.9	1055.4
338.15	988.1	1003.0	1022.1	1037.4	1051.7
343.15	984.1	999.6	1018.6	1033.7	1047.4

0.006, $u(T) = \pm 0.012$ K, $u(c) = 0.065$ mPa·s, $u(w) = \pm 2 \times 10^{-4}$ kg, $u(\alpha) = \pm 0.005$ mol CO_2/mol amine and $u(rep) = \pm 0.008$ mPa·s. The combined standard uncertainty for the viscosity measurement was calculated as $u(\eta) = \pm 0.067$ mPa·s^{-1}. Then the combined expanded uncertainty of the viscosity measurement $U(\eta)$ was found as $= \pm 0.135$ mPa·s (level of confidence = 0.95).

4. Results and discussion

This section is mainly divided into two sections to discuss the measured densities and viscosities of the AMP + MEA + H_2O + CO_2 mixtures. The proposed density and viscosity correlations to represent the data are discussed in relevant sections. The performance of the correlations are evaluated using two deviation factors of absolute average relative deviation (AARD%) and absolute maximum deviation (AMD) as given in Eqs. (1) and (2),

Average Absolute Relative Deviation:

$$AARD\ (\%) = \frac{100\%}{N}\sum_{i=1}^{N}\left|\frac{Y_i^E - Y_i^C}{Y_i^E}\right| \tag{1}$$

Absolute Maximum Deviation:

$$AMD = MAX\left|Y_i^E - Y_i^C\right| \tag{2}$$

where N, Y_i^E, and Y_i^C are referred to the number of data, the measured property and calculated property respectively.

Table 7
Density ρ/kg·m^{-3} of CO_2 loaded 27 mass % AMP + 3 mass % MEA + 70 mass % H_2O at different temperatures and CO_2 loadings (α/mol CO_2·mol amine^{-1}).

α/(mol CO_2·mol amine^{-1})	0.072	0.152	0.246	0.461	0.511
x_4	0.0059	0.0125	0.0200	0.0369	0.0407
T/K	ρ/kg·m^{-3}				
293.15	1013.5	1031.4	1042.2	1066.2	1078.0
298.15	1011.1	1028.7	1039.3	1062.8	1074.5
303.15	1008.4	1025.7	1036.2	1059.3	1071.0
308.15	1005.5	1022.9	1032.9	1055.7	1067.3
313.15	1002.6	1019.8	1029.6	1052.1	1063.7
318.15	999.6	1016.6	1026.3	1048.5	1060.1
323.15	996.3	1013.3	1022.6	1044.8	1056.4
328.15	993.2	1009.9	1019.4	1041.1	1052.7
333.15	989.8	1006.4	1015.9	1037.3	1048.9
338.15	986.2	1002.9	1012.0	1033.3	1045.2
343.15	982.8	999.3	1008.5	1029.7	1041.5

4.1. Density (ρ) and excess molar volume (V^E) of the AMP (1) + MEA (2) + H_2O (3) + CO_2 (4) mixtures

The density of pure AMP is available in literature [24–27]. Table 2 provides an overview of density of pure AMP measured in this study with the literature. The measured density in this study is in good accuracy with literature as the AARD showed <0.5% and AMD was 4.3 kg·m^{-3}. The deviations may arise due to the impurity of the material, measuring method and uncertainty of the temperature control. The comparison between literature and measured data indicated that the measuring system was calibrated properly for the density measurements. Measured density for AMP + MEA + H_2O by Mandal, et al. [14] and Li and Lie [15] are in good agreement with measured densities in this study indicating 2.6 kg·m^{-3} and 1.2 kg·m^{-3} of maximum deviations respectively.

The measured densities of the CO_2 unloaded amine mixture under different AMP and MEA mass % over the temperature range from 293.15 K to 343.15 K are listed in Table 3. Density has increased with the increase of MEA mole fraction in the mixture and has decreased with the increase of temperature. The excess molar volume V^E was calculated using measured density data of the aqueous amine mixtures as given in Eq. (3). A Redlich and Kister [16] type polynomial was fitted to excess molar volumes of aqueous mixtures as shown in Eq. (4), (5) and (6). This approach was adopted by authors [14,15,28] to represent excess molar volumes of ternary mixtures. Table 4 lists the required parameters of the binary pairs for the correlation to represent $10^6 \cdot V^E$. The correlation is in good agreement with measured densities as the AARD for the density of aqueous amine mixtures is 0.02% and AMD is 0.04 kg·m^{-3} and a comparison between measured densities and correlation is shown in Fig. 2.

$$\rho_{unloaded} = \frac{\sum_1^3 x_i M_i}{V^E + \sum_1^3 \frac{x_i M_i}{\rho_i}} \tag{3}$$

where $\rho_{unloaded}$, ρ_i, x_i, $M_i$and V^E represent the density of CO_2 unloaded aqueous mixture, density of pure component, mole fraction, molecular weights of AMP ($i = 1$), MEA ($i = 2$) and H_2O ($i = 3$) and excess molar volume respectively.

The excess molar volume of AMP + MEA + H_2O mixtures of the ternary system is assumed to be

$$V^E = V_{12}^E + V_{23}^E + V_{13}^E \tag{4}$$

$$V_{jk}^E = x_j x_k \sum_{i=0}^{n} A_i (x_j - x_k)^i \tag{5}$$

$$A_i = a + b(T) + c(T)^2 \tag{6}$$

where A_i are pair parameters and are assumed to be temperature dependent.

For the considered mole fractions and temperatures, V^E is negative. The V^E can be negative for two reasons, stronger intermolecular interactions like H-bond between unlike molecules and geometrical fitting due to the structural differences of the molecules giving negative contribution for V^E [29–31]. The variation of V^E with solution temperature is in such a way that the negative value of V^E decreases with increase of temperature for all considered mole fractions. This can be due to the weakening of molecular interactions at higher temperatures in which increased thermal energy of molecules decrease the interaction strength [32].

The increase of dissolved CO_2 concentration increases the density of AMP + MEA + H_2O + CO_2 mixtures. Tables 5, 6 and 7 list measured densities of AMP + MEA + H_2O + CO_2 mixtures with relevant CO_2 loadings and temperatures. The mole fraction of CO_2 as given by x_4 was calculated from the CO_2 loadings. In real mixtures, the dissolved CO_2 is in the form of carbamates, bicarbonates and

Table 8
Parameters of the Setschenow-type correlation (Eq. (7)) for the density of AMP + MEA + H_2O + CO_2 mixtures with relevant AARD (%) and AMD.

CO_2 loaded - 21% AMP 9% MEA 70% H_2O		AARD (%)	AMD ($kg \cdot m^{-3}$)
$a_{0,0}/(-) = 0.6433 \pm 0.0115$ $a_{0,1}/(K^{-1}) = (3.812 \pm 0.035) \cdot 10^{-3}$	$a_{1,0}/(-) = 23.4 \pm 1.1$ $a_{1,1}/(K^{-1}) = -0.0748 \pm 0.0035$	0.09	2.8
CO_2 loaded - 24% AMP 6% MEA 70% H_2O		AARD (%)	AMD ($kg \cdot m^{-3}$)
$a_{0,0}/(-) = 0.89 \pm 0.02$ $a_{0,1}/(K^{-1}) = 0.003 \pm 0.0003$	$a_{1,0}/(-) = 24.47 \pm 2.25$ $a_{1,1}/(K^{-1}) = -0.0818 \pm 0.0065$	0.08	2.11
CO_2 loaded - 27% AMP 3% MEA 70% H_2O		AARD (%)	AMD ($kg \cdot m^{-3}$)
$a_{0,0}/(-) = 2.376 \pm 0.017$ $a_{0,1}/(K^{-1}) = (-6.204 \pm 0.85) \cdot 10^{-05}$	$a_{1,0}/(-) = -3.7 \pm 0.4$ $a_{1,1}/(K^{-1}) = -0.03917 \pm 0.00135$	0.19	4.2

carbonates. This approach is efficient to develop correlations adopted by authors [33,34].

Several empirical correlations have been discussed in the literature for the density of amine + H_2O + CO_2 mixtures and the correlation proposed by Weiland, et al. [17] is highly discussed. The correlation was initially developed for the mixtures with one amine and parameters were found by fitting the density data at 298.15 K. Han, et al. [19] modified the original Weiland's correlation in order to fit the measured density data at different temperatures. Hartono, et al. [33] also proposed a correlation for density of MEA + H_2O + CO_2 mixtures that is capable to fit data at different temperatures. Shokouhi, et al. [35] adopted a modified Setschenow-type correlation [36,37] to fit the measured physical properties of CO_2 loaded aqueous amine mixtures including more than one amine in the mixture. In this study, a modified Setschenow-type correlation and a modified Weiland's correlation is used to represent the measured densities.

Setschenow-type correlation for density:

$$\ln\left(\frac{\rho}{\rho_0}\right) = (a_{0,0} + a_{0,1}T)x_4 + (a_{1,0} + a_{1,1}T){x_4}^2 \tag{7}$$

where ρ/ρ_0 represent the ratio between density of CO_2 loaded and unloaded mixtures at equivalent temperatures. Parameters $a_{i,j}$, x_4 and T indicate temperature dependent parameters, CO_2 mole fraction and temperature in the liquid mixture. The parameters $a_{i,j}$ were found by fitting measured densities to the correlation and values are listed in Table 8 with the relevant amine concentrations in the aqueous mixtures.

Table 9
Correlation parameters of the modified Weiland's density correlation.

Parameters		Values
V_4	$a_0/(m^3 \cdot mol^{-1})$	-20.9 ± 0.6
	$a_1/(m^3 \cdot mol^{-1} \cdot K^{-1})$	0.25 ± 0.01
	$a_2/(m^3 \cdot mol^{-1} \cdot K^{-2})$	-0.0011 ± 0.00045
	$a_3/(m^3 \cdot mol^{-1} \cdot K^{-3})$	$(-5 \pm 2) \cdot 10^{-6}$
V^*	$b_0/(m^3 \cdot mol^{-1})$	-325.65 ± 3.25
	$b_1/(m^3 \cdot mol^{-1} \cdot K^{-1})$	-0.892 ± 0.095
	$b_2/(m^3 \cdot mol^{-1} \cdot K^{-2})$	0.032 ± 0.006
	$b_3/(m^3 \cdot mol^{-1} \cdot K^{-3})$	-0.0002 ± 0.0001
c	$c_0/(m^3 \cdot mol^{-1})$	$3{,}875{,}900 \pm 250$
	$c_1/(m^3 \cdot mol^{-1} \cdot K^{-1})$	$-32{,}342.6 \pm 1.5$
	$c_2/(m^3 \cdot mol^{-1} \cdot K^{-2})$	87.277 ± 0.005
	$c_3/(m^3 \cdot mol^{-1} \cdot K^{-3})$	-0.0735 ± 0.0002
d	$d_0/(m^3 \cdot mol^{-1})$	$-48{,}040{,}000 \pm 7500$
	$d_1/(m^3 \cdot mol^{-1} \cdot K^{-1})$	$406{,}200 \pm 25$
	$d_2/(m^3 \cdot mol^{-1} \cdot K^{-2})$	-1107.27 ± 0.15
	$d_3/(m^3 \cdot mol^{-1} \cdot K^{-3})$	0.9415 ± 0.0003
e	$e_0/(m^3 \cdot mol^{-1})$	$(-5481.4 \pm 4.7) \cdot 10^4$
	$e_1/(m^3 \cdot mol^{-1} \cdot K^{-1})$	$481{,}977 \pm 170$
	$e_2/(m^3 \cdot mol^{-1} \cdot K^{-2})$	-1388.65 ± 0.28
	$e_3/(m^3 \cdot mol^{-1} \cdot K^{-3})$	1.292 ± 0.002

Modified Weiland's density correlation:

$$\rho = \frac{\sum_{i=1}^{4} x_i M_i}{V} \tag{8}$$

$$V = \sum_{i=1}^{3} x_i V_i + (x_4 V_4 + x_1 x_2 x_3 V^* + x_1 x_2 x_4 V^{**}) \cdot 10^{-6} \tag{9}$$

$$V^{**} = c + dx_1 + ex_2 \tag{10}$$

where V_i, V, ρ, M_i and x_i are molar volumes of pure amine, molar volume of mixture, density of CO_2 loaded mixture, molecular weight of components and mole fraction of components in the mixture. The subscript $i = 1$, 2, 3 and 4 refer to AMP, MEA, H_2O and CO_2 respectively. The molar volumes of pure AMP at different temperatures were determined by the measured density data listed in Table 2. For pure MEA, the data reported by Han, et al. [19] and for pure H_2O data from IAPWS [38] were adopted to obtain molar volumes. The missing density data at low temperatures of AMP and MEA were found by fitting a second order polynomial to available measured densities. V_4, V^*, c, d,and e are fitting parameters including temperature as an independent variable to correlate the dependency of density on temperature.

$$V_4 = a_0 + a_1(T - 273.15) + a_2(T - 273.15)^2 + a_3(T - 273.15)^3 \tag{11}$$

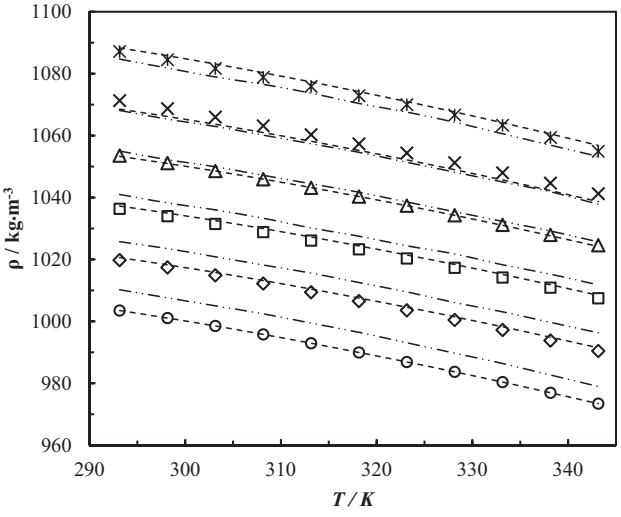

Fig. 3. Density of CO_2 loaded 21 mass % AMP + 9 mass % MEA + 70 mass % H_2O at different temperatures and CO_2 loadings (α/mol CO_2·mol amine^{-1}): 0.000, 'O'; 0.107, '◇'; 0.210, '□'; 0.308, '△'; 0.400, 'x'; 0.518, '*'. Correlations: Setschenow-type, '- - -'; Modified Weiland's, '_ · · _'.

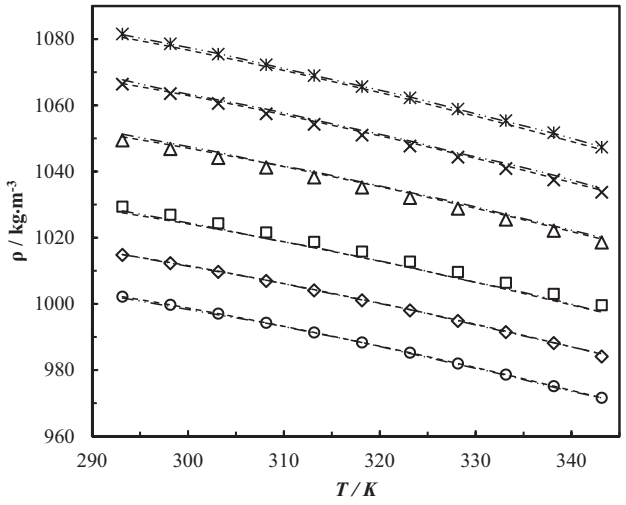

Fig. 4. Density of CO_2 loaded 24 mass % AMP + 6 mass % MEA + 70 mass % H_2O at different temperatures and CO_2 loadings (α/mol CO_2·mol amine^{-1}): 0.000, '○'; 0.083, '◇'; 0.165, '□'; 0.314, '△'; 0.418, 'x'; 0.508, '⁎'. Correlations: Setschenow-type, '- - -'; Modified Weiland's, '_ ·· _'.

$$V^{*} = b_0 + b_1(T-273.15) + b_2(T-273.15)^2 + b_3(T-273.15)^3 \quad (12)$$

$$c = c_0 + c_1(T) + c_2(T)^2 + c_3(T)^3 \quad (13)$$

$$d = d_0 + d_1(T) + d_2(T)^2 + d_3(T)^3 \quad (14)$$

$$e = e_0 + e_1(T) + e_2(T)^2 + e_3(T)^3 \quad (15)$$

The values of the fitted parameters from Eq. (9) to Eq. (15) are presented in Table 9.

The measured densities compared with the Setschenow-type correlation and the modified Weiland correlation are shown in Figs. 3, 4 and 5. The correlations are fitted with satisfactory accuracies and Table 8 provides calculated AARD and AMD for the Setschenow-type correlation. The advantage of the modified Weiland's density correlation is that a single correlation is applicable to the entire range of AMP, MEA, H_2O and CO_2 considered in the study with AARD and AMD with 0.42% and 13.7 kg·m^{-3} respectively. The Setschenow-type correlation show better agreement with measured densities; nevertheless, both correlations are acceptable to use in engineering calculations.

Table 10
Experimental data of the viscosity η/mPa·s of pure AMP from this work and literature at different temperatures.

T/K	η/mPa·s		
	This work	Literature	
		Henni, et al. [25]	Li and Lie [15]
303.15			99.4748
313.15	48.477	47.80	46.9258
318.15	35.161		
323.15	26.001	25.10	24.2108
328.15	19.524		
333.15	15.004	14.40	13.9977
338.15	11.705		
343.15	9.269	8.91	8.6418
348.15	7.482		
353.15	6.109		5.6485
358.15	5.055		
363.15	4.227		

4.2. Viscosity and free energy of activation for viscus flow of AMP (1) + MEA (2) + H_2O (3) + CO_2 (4) mixtures

The viscosity of pure AMP was measured and compared in Table 10 with available data in literature. From Fig. 6, it can be seen that measured viscosities for pure AMP and MEA are in good agreement with literature [15,21,25,39]. The data were correlated according to the modified Andrade viscosity model [40] by Vogel [41] as shown in Eq. (16). The correlation was able to fit the measured viscosities with acceptable accuracies and calculated parameters are shown in Table 11. Measured viscosity for AMP + MEA + H_2O by Mandal, et al. [14] and Li and Lie [15] are in good agreement with measured viscosities in this study indicating

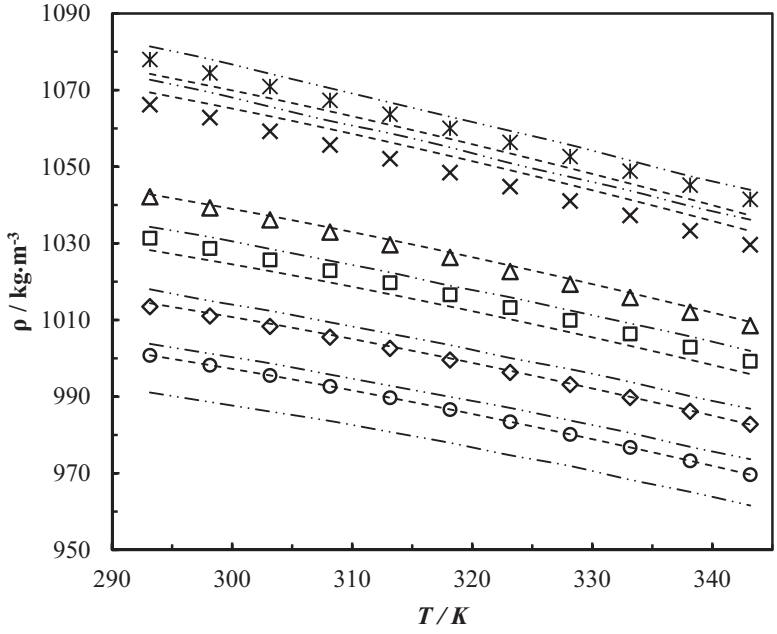

Fig. 5. Density of CO_2 loaded 27 mass % AMP + 3 mass % MEA + 70 mass % H_2O at different temperatures and CO_2 loadings (α/mol CO_2·mol amine^{-1}): 0.000, '○'; 0.072, '◇'; 0.152, '□'; 0.246, '△'; 0.461, 'x'; 0.511, '⁎'. Correlations: Setschenow-type, '- - -'; Modified Weiland's, '_ ·· _'.

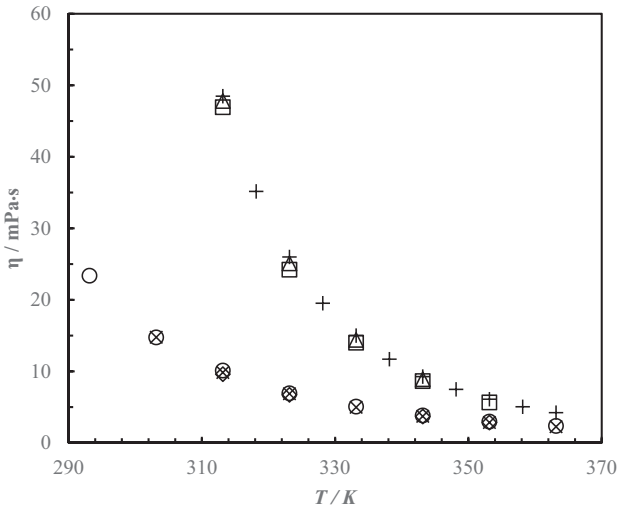

Fig. 6. Viscosity of pure amines. Pure AMP: this study, '+'; Henni, et al. [25], '△'; Li and Lie [15], '□'. Pure MEA: this study, '○'; Idris, et al. [21], 'x'; Amundsen, et al. [39], '◇'.

0.32 mPa·s and 0.02 of maximum deviations respectively. Viscosities measured by Mandal, et al. [14] showed a small discrepancy compared to this study at low temperatures around 293.15 K as illustrated in Figs. S1, S2 and S3 in the Supplementary materials.

$$\ln(\eta) = a + \frac{b}{T + c} \tag{16}$$

(See Figs. 6–12.)

The measured viscosities of AMP + MEA + H_2O + CO_2 mixtures are listed in Tables 12, 13 and 14. Viscosity increased with the increase of dissolved CO_2 in the solution and this was observed in all the different amine mixtures considered in this study. Viscosity decreases with increasing temperature in all mixtures with different amine and CO_2 concentrations. The presence of CO_2 in the mixtures forms ionic products of carbamates and bicarbonate that increases the intermolecular interactions, which results in higher viscosities than aqueous amine mixtures without CO_2. Fu, et al. [42] presented viscosity data for AMP + MEA + H_2O + CO_2 mixtures at different AMP and MEA concentrations, total amine concentrations and CO_2 loadings compared to this work. Fig. S4 provides a summary of measured viscosity in this work with viscosity reported by Fu, et al. [42].

The measured viscosity and density of aqueous amine solutions were considered to calculate free energy of activation for viscous flow as described by Eyring [18]. For Newtonian fluids, Eyring's viscosity model relates viscosity and molar volume with free energy of activation of viscous flow as shown in Eq. (17). Viscosity measurements under different shear rates confirm the Newtonian behavior of solutions. Eyring [18] explains that the fluid at rest continuously undergoes rearrangements. The term ΔG^* in Eq. (17) refer the free energy of activation for viscous flow to jump a molecule from its cage into an adjacent hole by overcoming the potential barrier [43].

$$\eta = \frac{hN_A}{V} exp\left(\frac{\Delta G^*}{RT}\right) \tag{17}$$

Table 11
Regression parameters, AARD (%) and AMD for correlation given in Eq. (16).

Parameter	Value	AARD (%)	AMD (mPa·s)
a/(−)	−4.791 ± 0.002	0.23	0.23
b/(K)	1105 ± 1		
c/(K)	−185.8 ± 0.1		

where ΔG^*, η, V, h, N_A, R and T refer to the free energy of activation for viscous flow ($J \cdot mol^{-1}$), viscosity ($Pa \cdot s$), molar volume ($m^3 \cdot mol^{-1}$), Planck's constant ($m^2 \cdot kg \cdot s^{-1}$), Avogadro number ($mol^{-1}$), gas constant ($J \cdot mol^{-1} \cdot K^{-1}$) and temperature (K). Considering the Eyring's viscosity model for both real and ideal mixtures following Eq. (18) and Eq. (19) are derived and excess free energy of activation for viscous flow ΔG^{E*} is introduced. The sign of ΔG^{E*} alone with V^E carries valuable information about viscosity and intermolecular attractions among the components of mixture compared to an ideal mixture

$$\ln(\eta V) = \ln(\eta V)_{ideal} + \frac{\Delta G^{E*}}{RT} \tag{18}$$

$$\ln(\eta V) = \sum_i x_i \ln\left(\eta_i V_i^0\right) + + \frac{\Delta G^{E*}}{RT} \tag{19}$$

The calculated ΔG^{E*} gives positive values for density and viscosity data presented by Mandal, et al. [14]. This reveals the presence of strong molecular interactions like H-bonds among the unlike molecules [44–47].The calculated viscosity deviation η^E as shown in Eq. (20) gives negative values over the amine concentration and temperature range. The negative sign for η^E indicates weak molecular interactions compared to the pure liquids. The molecular interaction is not the only factor that causes viscosity deviation of liquid mixtures [47]. In the analysis of liquid mixtures, aspects of molecular size and shape of the components, size of the intermolecular complexes and dispersion forces are also equally significant [44,45,47–49].

$$\eta^E = \eta - \sum_{i=1}^{n} x_i \eta_i \tag{20}$$

The calculated excess free energy of activation for viscous flow for unloaded aqueous amine mixtures are correlated using a Redlich-Kister polynomial with temperature dependency.

The excess free energy of activation for viscous flow of AMP + MEA + H_2O mixtures of the ternary system is assumed to be

$${}^{\Delta G}E*/_{RT} = \Delta G_{12}^{E*} + \Delta G_{23}^{E*} + \Delta G_{13}^{E*} \tag{21}$$

$$\Delta G_{jk}^{E*} = x_j x_k \sum_{i=0}^{n} A_i (x_j - x_k)^i \tag{22}$$

$$A_i = a + b(T) + c(T)^2 \tag{23}$$

The proposed correlation was able to represent measured viscosities by Mandal, et al. [14] with <2% AARD of accuracy using Eq. (19) and correlation parameters are listed in Table 15.

The approaches based on a Setschenow-type correlation, a Weiland's viscosity correlation and Eyring's viscosity model were adopted to fit the viscosities of AMP + MEA + H_2O + CO_2 mixtures and illustrated in Figs. 7-12. Three Setschenow-type correlations were proposed as given in Eq. (24) for each mixture with different amine concentrations. As illustrated in Eq. (25), the original Weiland's viscosity correlation was modified to fit viscosity data for mixtures with more than one amine. The free energy of activation for viscous flow in Eyring's viscosity model was calculated from the measured viscosity and density data and was correlated with the proposed expression as shown in Eq. (26) and Eq. (27).

Setschenow-type correlation for viscosity:

The viscosity of AMP + MEA + H_2O + CO_2 mixtures was correlated according to the Setschenow-type correlation as shown in Eq. (24).

$$\ln\left(\frac{\eta}{\eta_0}\right) = (a_{0,0} + a_{0,1}T)x_4 + (a_{1,0} + a_{1,1}T)x_4^2 + (a_{2,0} + a_{2,2}T)x_4^3 \tag{24}$$

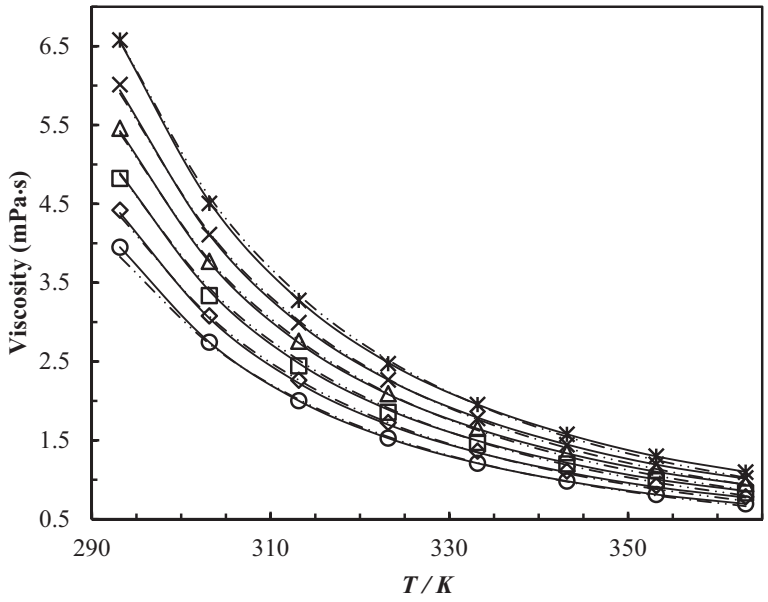

Fig. 7. Viscosity of CO_2 loaded 21 mass % AMP + 9 mass % MEA + 70 mass % H_2O at different temperatures and CO_2 loadings (α/mol CO_2·mol amine^{-1}): 0.000, '○'; 0.107, '◇'; 0.210, '□'; 0.308, '△'; 0.400, 'x'; 0.518, '⁎'. Correlations: Setschenow-type, '———'; Modified Weiland's, '_ ·· _'.

where η/η_0 represent the ratio between viscosity of CO_2 loaded and unloaded mixtures at equivalent temperatures. Parameters $a_{i,j}$, x_4 and T indicate temperature dependent parameters, CO_2 mole fraction and temperature in the liquid mixture.

Table 16 lists the calculated parameters, AARD and AMD for Setschenow-type correlation for different mixtures. It reveals that the correlation is capable of fitting viscosities with acceptable accuracy. Viscosity deviation is high at low temperatures and a maximum deviation was observed at 293.15 K.

Modified Weiland's viscosity correlation:

The original Weiland's viscosity correlation [17] was made for the mixtures of amine + H_2O + CO_2 with single amine in which the CO_2 loading was considered as an independent variable. A new fitting parameter with amine mole fractions was considered to fit the viscosities and CO_2 mole fraction in the mixtures were considered instead of CO_2 loading as shown in Eq. (25).

$$\frac{\eta}{\eta_{H_2O}} = \exp\left[\frac{[(ax_1 + bx_2 + c)T + (dx_1 + ex_2 + f)]\left[x_4(gx_1 + hx_2 + iT + j) + 10^3\right](x_1 + x_2)}{T^2}\right] \tag{25}$$

where η, η_{H2O}, x_4 and T are viscosity of CO_2 loaded mixture, viscosity of H_2O, mole fraction of CO_2 and temperature of the liquid mixture.

The parameters shown in Eq. (25) are given in Table 17. The Weiland's viscosity correlation can be written in a form of $\eta_{Co2loaded}/\eta_{H2O} = \exp(f(w)g(\alpha)/T)$ where the function $f(w)$ was determined from CO_2 unloaded solution data. Here, instead of using data from CO_2

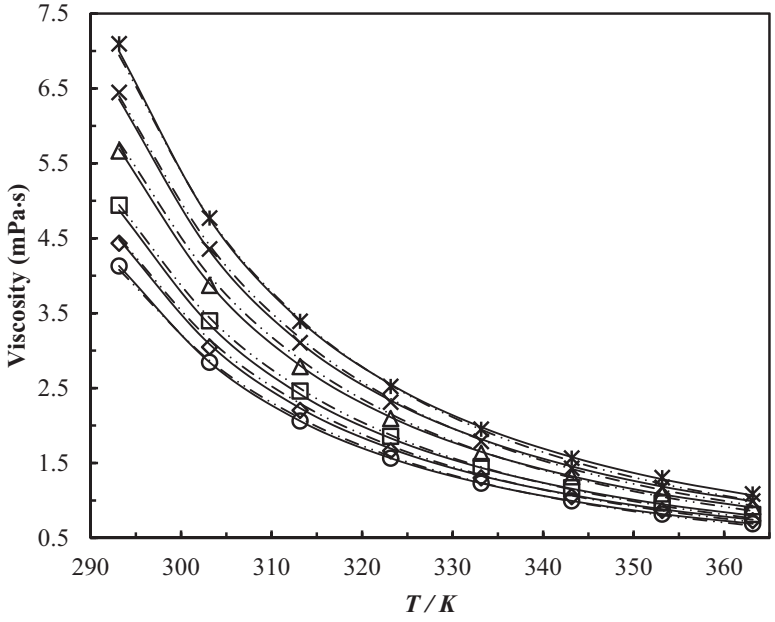

Fig. 8. Viscosity of CO_2 loaded 24 mass % AMP + 6 mass % MEA + 70 mass % H_2O at different temperatures and CO_2 loadings (α/mol CO_2·mol amine^{-1}): 0.000, '○'; 0.083, '◇'; 0.165, '□'; 0.314, '△'; 0.418, 'x'; 0.508, '⁎'. Correlations: Setschenow-type, '———'; Modified Weiland's, '_ ·· _'.

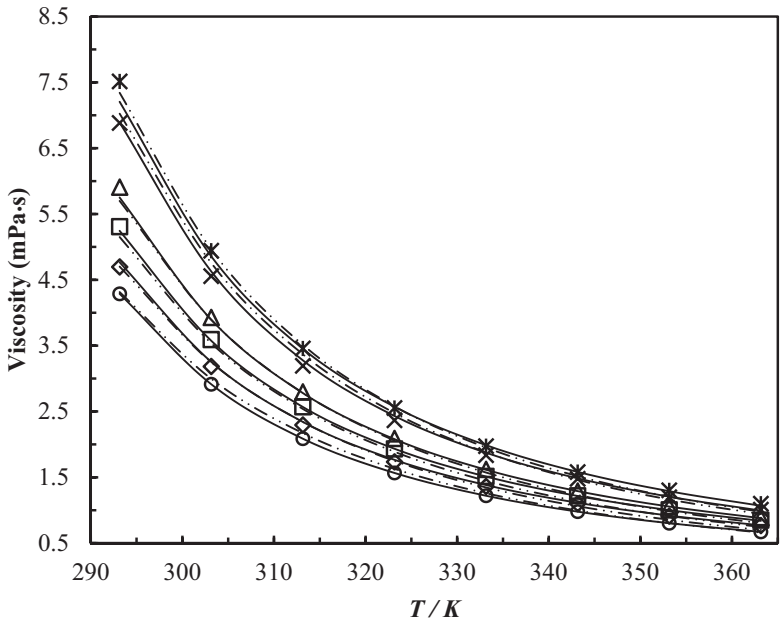

Fig. 9. Viscosity of CO_2 loaded 27 mass % AMP + 3 mass % MEA + 70 mass % H_2O at different temperatures and CO_2 loadings (α/mol CO_2·mol amine^{-1}): 0.000, '○'; 0.072, '◇'; 0.152, '□'; 0.246, '△'; 0.461, 'x'; 0.511, '⁎'. Correlations: Setschenow-type, '———'; Modified Weiland's, '_ ·· _'.

unloaded solutions, the information related to CO_2 loaded solutions was adopted for the data fit. The calculated AARD and AMD as given in the Table 17 indicate that correlated viscosities are in good agreement with the measured viscosities and useful in engineering calculations.

Correlation based on Eyring's viscosity model.

The calculated free energy of activation for viscous flow ΔG^* from measured densities and viscosities for AMP + MEA + H_2O + CO_2 mixtures was correlated as given in Eq. (26) and Eq. (27). The ΔG^* increases with the increase of CO_2 loading and decreases with increasing temperature. Matin, et al. [50], described the variations in viscosity with CO_2 loading relating to the solution ionic strength and pH. Increase of CO_2 loading reduce the pH while increasing the ionic strength. The measured pH versus CO_2 loading is presented in Fig. S5. The presence of CO_2 in an amine + H_2O mixture creates a pool of cations and anions including carbamate ($RNHCO_2^-$), protonated amine (RNH_3^+), bicarbonate (HCO_3^-), carbonate (CO_3^{2-}), $OH^-$and H^+ ions increase the ionic strength and intermolecular interactions that leads to high viscosity.

$$\ln(\eta V)_{CO_2 loaded} = \ln(\eta V)_{unloaded} + f(x_1, x_2, x_4, T) \quad (26)$$

$$f(x_1, x_2, x_4, T) = x_4(k_1 + k_2 T + k_3 x_4)(k_4 x_1 + k_5 x_2 + k_6) \quad (27)$$

where x_i and T are mole fraction and temperature. The subscript $i = 1, 2,$ and 4 refers to AMP, MEA and CO_2 respectively. The function f determines the property of $(\Delta G^*_{CO2loaded} - \Delta G^*_{unloaded})/RT$ where $\Delta G^*_{CO2loaded}$ and $\Delta G^*_{unloaded}$ refer to free energy of activation for viscous flow for CO_2 loaded and unloaded solutions respectively.

The calculated parameters for the correlation based on Eyring's viscosity model is given in Table 18 with calculated AARD and AMD. The data fit is limited to 343.15 K temperature due to the availability of densities of the mixtures. The correlation is recommended for use in engineering calculation as the AARD is acceptable. The main drawback of this approach is that it requires density data for the viscosity calculations.

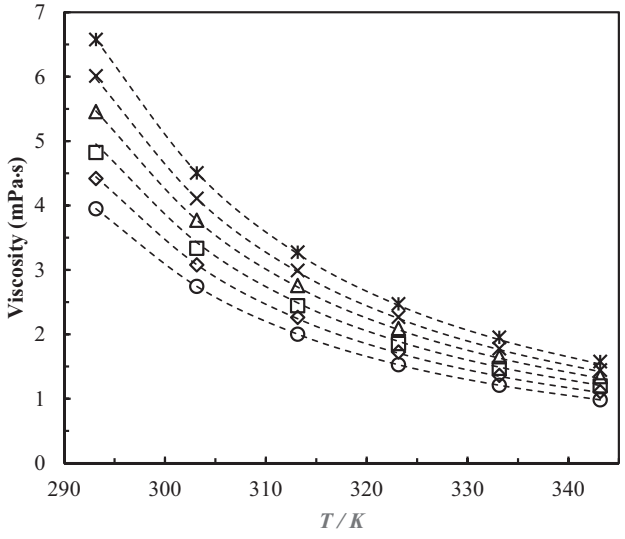

Fig. 10. Viscosity of CO_2 loaded 21 mass % AMP + 9 mass % MEA + 70 mass % H_2O at different temperatures and CO_2 loadings (α/mol CO_2·mol amine^{-1}): 0.000, '○'; 0.107, '◇'; 0.210, '□'; 0.308, '△'; 0.400, 'x'; 0.518, '⁎'. Correlation: '- - -'.

Table 12
Viscosity of CO_2 loaded 21 mass % AMP + 9 mass % MEA + 70 mass % H_2O at different temperatures and CO_2 loadings (α/mol CO_2·mol amine^{-1}).

α/(mol CO_2·mol amine^{-1})	0.000	0.107	0.210	0.308	0.400	0.518
x_4	0.0000	0.0095	0.0185	0.0269	0.0346	0.0444
T/K	η/mPa·s					
293.15	3.949	4.419	4.822	5.458	6.012	6.577
303.15	2.744	3.078	3.336	3.771	4.109	4.506
313.15	2.002	2.262	2.443	2.757	2.992	3.275
323.15	1.527	1.725	1.857	2.091	2.267	2.472
333.15	1.209	1.363	1.472	1.651	1.778	1.953
343.15	0.982	1.110	1.200	1.343	1.445	1.576
353.15	0.812	0.924	0.987	1.120	1.197	1.298
363.15	0.693	0.784	0.831	0.947	1.022	1.097

Table 13
Viscosity of CO_2 loaded 24 mass % AMP + 6 mass % MEA + 70 mass % H_2O at different temperatures and CO_2 loadings (α/mol CO_2·mol amine^{-1}).

α/(mol CO_2·mol amine^{-1})	0.000	0.083	0.165	0.314	0.418	0.508
x_4	0.0000	0.0071	0.0141	0.0264	0.0349	0.0420
T/K	η/mPa·s					
293.15	4.130	4.435	4.941	5.666	6.448	7.096
303.15	2.845	3.048	3.399	3.872	4.358	4.770
313.15	2.061	2.203	2.461	2.788	3.106	3.392
323.15	1.565	1.663	1.857	2.094	2.313	2.523
333.15	1.231	1.302	1.452	1.632	1.789	1.952
343.15	0.995	1.052	1.171	1.318	1.431	1.566
353.15	0.819	0.868	0.968	1.089	1.176	1.305
363.15	0.690	0.729	0.813	0.918	0.992	1.088

Table 15
Binary parameters A_0, A_1 and $A_2$of the equation $\Delta G^{E*}_{jk} = x_j x_k \sum_{i=0}^{n} A_i (x_j - x_k)^i$for excess free energy of activation for viscous flow for AMP (1) + MEA (2) + H_2O (3).

Parameters		Binary pair		
		AMP + MEA	MEA + H_2O	AMP + H_2O
A_0	a/(−)	−42,410 ± 10	−3003.3 ± 1.0	−8202.5 ± 0.2
	b/(K^{-1})	−93.83 ± 0.05	−31.660 ± 0.005	14.1692 ± 0.0005
	c/(K^{-2})	−0.5972 ± 0.0002	0.02027 ± 0.00001	0.333114 ± 0.000002
A_1	a/(−)	−168,639 ± 250	4561 ± 1	−6020.9 ± 0.2
	b/(K^{-1})	1528 ± 1	−24.420 ± 0.003	9.6437 ± 0.0005
	c/(K^{-2})	−4.464 ± 0.002	0.52729 ± 0.00002	0.552341 ± 0.000002
A_2	a/(−)	6,476,811 ± 2500	11,567 ± 1	4014.5 ± 0.3
	b/(K^{-1})	−43,939 ± 10	24.233 ± 0.004	−5.4479 ± 0.0008
	c/(K^{-2})	74.26 ± 0.03	0.62877 ± 0.00002	0.180252 ± 0.000003

The enthalpy of activation for viscous flow $\Delta H^*$and entropy activation for viscous flow ΔS^*were determined using rearranged Eyring's viscosity model as given in Eq. (28). The slope and the intercept of the linear relationship of $R \ln (\eta V/hN_A)$ vs $1/T$ provide information about ΔH^* and ΔS^*. Tables 19 and 20 list the calculated ΔG^*, ΔH^* and ΔS^* of the mixtures at different CO_2 loadings and temperatures.

$$Rln\left(\frac{\eta V}{hN_A}\right) = \frac{\Delta H^*}{T} - \Delta S^* \tag{28}$$

$$\Delta G^* = \Delta H^* - T\Delta S^* \tag{29}$$

The results reveal that ΔG^* ΔH^* and $\Delta S^*$are positive for all considered mixtures while ΔH^* is greater than $T\Delta S^*$. This indicates that the contribution of enthalpy of activation to the free energy of activation is greater than entropy of activation for viscous flow. For the aqueous mixtures, ΔG^* increases with the increase of AMP concentration indicating that AMP has a higher effect on molecular interactions than MEA. For CO_2 loaded solutions, the mixture becomes an electrolyte with strong molecular interactions compared to an aqueous mixture, which is reflected by high ΔG^*.

5. Conclusion

This study discusses the densities and viscosities of unloaded and CO_2 loaded AMP + MEA + H_2O mixtures at different amine concentrations, CO_2 loadings and temperatures. The amine mass % of AMP and MEA were 21/9, 24/6 and 27/3 by maintaining 70 mass % of H_2O in the aqueous solutions. The CO_2 loadings of mixtures were maintained at different levels in which maximum is <0.6 (mol CO_2·mol amine^{-1}).

The densities of mixtures were measured in the temperature range from 293.15 K to 343.15 K. Density increases with the increase of CO_2 loading and decreases with temperature. The measured density data were fit into a Setschenow-type correlation with 0.09%, 0.08% and 0.19% AARD and 2.8 kg·m^{-3}, 2.21 kg·m^{-3} and 4.2 kg·m^{-3} AMD for mixtures of 21/9, 24/6 and 27/3 of AMP mass %/MEA mass % respectively. The Weiland's density correlation was modified to fit density data of CO_2 loaded aqueous mixtures with more than one amine for the range of amine concentrations and temperatures. The correlation was capable to represent density data at 0.42% AARD and 13.7 kg·m^{-3} AMD. The accuracies of density data fit to the Setschenow-type correlation and modified Weiland's density correlation are regarded as satisfactory for correlations in engineering calculations.

The viscosities of mixtures were measured in the temperature range from 293.15 K to 363.15 K. Viscosity increases with increase of CO_2 loading and decreases with temperature. A Setschenow-type correlation was proposed to fit the measured viscosities and the accuracy of the data fit was calculated to 0.75%, 0.99% and 0.94% AARD and 0.07 mPa·s, 0.1 mPa·s and 0.31 mPa·s AMD for mixtures of 21/9, 24/6 and 27/3 of AMP mass %/MEA mass % respectively. A modified Weiland's viscosity correlation for CO_2 loaded aqueous mixtures with more than one amine was proposed to represent viscosity data. The accuracy of data fit was calculated to 2.7%

Table 14
Viscosity of CO_2 loaded 27 mass % AMP + 3 mass % MEA + 70 mass % H_2O at different temperatures and CO_2 loadings (α/mol CO_2·mol amine^{-1}).

α/(mol CO_2·mol amine^{-1})	0.000	0.072	0.152	0.246	0.461	0.511
x_4	0.0000	0.0059	0.0125	0.0200	0.0369	0.0407
T/K	η/mPa·s					
293.15	4.288	4.695	5.308	5.908	6.883	7.515
303.15	2.913	3.183	3.591	3.928	4.556	4.943
313.15	2.086	2.295	2.571	2.797	3.194	3.459
323.15	1.566	1.734	1.931	2.090	2.366	2.553
333.15	1.220	1.361	1.513	1.620	1.837	1.973
343.15	0.978	1.099	1.219	1.291	1.477	1.578
353.15	0.803	0.910	1.006	1.058	1.197	1.303
363.15	0.670	0.767	0.849	0.888	1.008	1.099

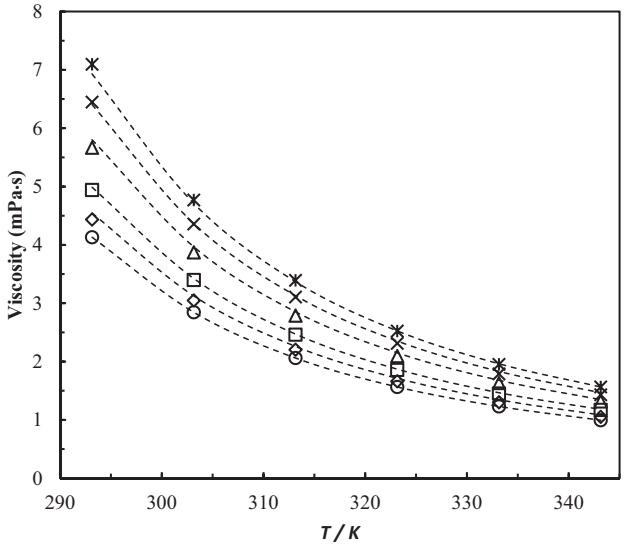

Fig. 11. Viscosity of CO_2 loaded 24 mass % AMP + 6 mass % MEA + 70 mass % H_2O at different temperatures and CO_2 loadings (α/mol CO_2·mol amine^{-1}): 0.000, '○'; 0.083, '◇'; 0.165, '□'; 0.314, '△'; 0.418, 'x'; 0.508, '⁎'. Correlation: '- - -'.

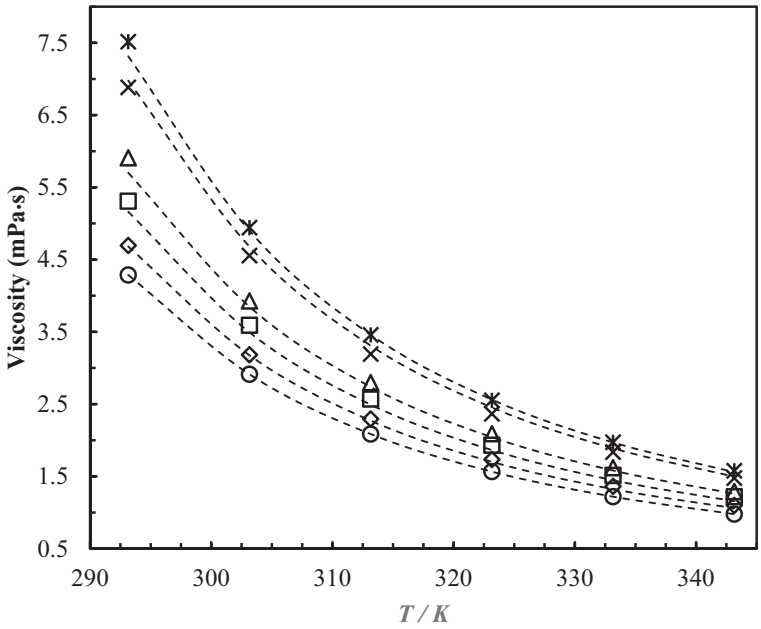

Fig. 12. Viscosity of CO_2 loaded 27 mass % AMP + 3 mass % MEA + 70 mass % H_2O at different temperatures and CO_2 loadings (α/mol CO_2·mol amine^{-1}): 0.000, '○'; 0.072, '◇'; 0.152, '□'; 0.246, '△'; 0.461, 'x'; 0.511, '⁎'. Correlation: '- - -'.

Table 16
Parameters of the Setschenow-type correlation (Eq. (24)) for the viscosity of AMP + MEA + H_2O + CO_2 mixtures with relevant AARD (%) and AMD.

CO_2 loaded - 21% AMP 9% MEA 70% H_2O			AARD (%)	AMD (mPa·s)
$a_{0,0}/(-) = 3.575 \pm 0.010$ $a_{0,1}/(K^{-1}) = (2.196 \pm 0.0045)\cdot 10^{-2}$	$a_{1,0}/(-) = 563.8 \pm 1.2$ $a_{1,1}/(K^{-1}) = -1.516 \pm 0.0045$	$a_{2,0}/(-) = -6516 \pm 130$ $a_{2,2}/(K^{-1}) = 15.49 \pm 0.45$	0.75	0.07
CO_2 loaded - 24% AMP 6% MEA 70% H_2O			AARD (%)	AMD (mPa·s)
$a_{0,0}/(-) = 13.7 \pm 0.01$ $a_{0,1}/(K^{-1}) = (-8.313 \pm 0.05)\cdot 10^{-3}$	$a_{1,0}/(-) = 299.2 \pm 2.5$ $a_{1,1}/(K^{-1}) = -0.895 \pm 0.008$	$a_{2,0}/(-) = -2727 \pm 275$ $a_{2,2}/(K^{-1}) = 8.75 \pm 0.95$	0.99	0.1
CO_2 loaded - 27% AMP 3% MEA 70% H_2O			AARD (%)	AMD (mPa·s)
$a_{0,0}/(-) = -22.45 \pm 0.03$ $a_{0,1}/(K^{-1}) = 0.1433 \pm 0.00012$	$a_{1,0}/(-) = 3157 \pm 6$ $a_{1,1}/(K^{-1}) = -11.86 \pm 0.02$	$a_{2,0}/(-) = (-5.298 \pm 0.0950)\cdot 10^{4}$ $a_{2,2}/(K^{-1}) = 193.5 \pm 3.3$	0.94	0.31

AARD and 0.2 mPa·s AMD for the considered amine concentration and temperature range.

The free energy of activation for viscous flow ΔG^* from Eyring's viscosity model showed that ΔG^* increases with the increase of CO_2 loading and decreases with the increase of temperature. The calculated properties of ΔG^*, $\Delta H^*$and ΔS^* increase with the increase of AMP concentration in the aqueous mixtures. The correlation developed based on Eyring's viscosity model was in good agreement with measured viscosity data showing an accuracy of the regression of 1.4% AARD and 0.2 mPa·s AMD.

CRediT authorship contribution statement

Sumudu S. Karunarathne: Writing - original draft, Investigation.**Dag A. Eimer:**Supervision.**Lars E. Øi:**Supervision.

Table 17
Parameters for modified Weiland's viscosity correlation.

Parameters	Value
a/(K)	−935.048 ± 0.015
b/(K)	−572.018 ± 0.025
c/(K)	68.8463 ± 0.0004
d/(K^2)	244,061 ± 1.6
e/(K^2)	136,460 ± 10
f/(K^2)	−16,162.22 ± 0.20
g/(−)	385,100 ± 163
h/(−)	257,300 ± 1013
i/(K^{-1})	−26.692 ± 0.035
j/(−)	−13,288 ± 12
AARD (%)	2.7
AMD (mPa·s)	0.2

Table 18
Parameters for correlation based on Eyring's viscosity model.

Parameters	Value
$k_1/(-)$	682.53 ± 1.05
$k_2/(K^{-1})$	−0.863 ± 0.004
$k_3/(-)$	−2443 ± 180
$k_4/(-)$	−1.4674 ± 0.0012
$k_5/(-)$	−1.2432 ± 0.0075
$k_6/(-)$	$(15.123 \pm 0.009)\cdot 10^{-2}$
AARD (%)	1.4
AMD (mPa·s)	0.2

Table 19
Free energy of activation for viscous flow ΔG^*/kJ·mol^{-1} for AMP (1) + MEA (2) + H_2O (3) + CO_2 (4) mixtures.

AMP/MEA mass %	α/mol CO_2·mol amine^{-1}	x_1	x_2	x_4	ΔG^*/kJ·mol^{-1}					
					293.15 K	303.15 K	313.15 K	323.15 K	333.15 K	343.15 K
21/9	0.000	0.0552	0.0345	0.0000	13.265	12.813	12.429	12.115	11.861	11.644
	0.107	0.0547	0.0342	0.0095	13.520	13.082	12.726	12.419	12.169	11.967
	0.210	0.0542	0.0339	0.0185	13.713	13.263	12.904	12.593	12.357	12.163
	0.308	0.0537	0.0336	0.0269	13.992	13.549	13.195	12.888	12.649	12.458
	0.400	0.0533	0.0333	0.0346	14.203	13.741	13.382	13.079	12.827	12.638
	0.518	0.0527	0.0330	0.0444	14.406	13.957	13.601	13.295	13.070	12.874
24/6	0.000	0.0633	0.0231	0.0000	13.386	12.916	12.518	12.194	11.925	11.696
	0.083	0.0629	0.0229	0.0071	13.544	13.074	12.674	12.339	12.062	11.836
	0.165	0.0624	0.0228	0.0141	13.787	13.327	12.940	12.612	12.339	12.114
	0.314	0.0616	0.0225	0.0264	14.100	13.634	13.243	12.914	12.640	12.428
	0.418	0.0611	0.0223	0.0349	14.393	13.911	13.503	13.159	12.873	12.641
	0.508	0.0606	0.0221	0.0420	14.607	14.118	13.712	13.371	13.093	12.878
27/3	0.000	0.0715	0.0116	0.0000	13.490	12.989	12.564	12.211	11.916	11.664
	0.072	0.0711	0.0115	0.0059	13.693	13.193	12.791	12.464	12.197	11.972
	0.152	0.0706	0.0114	0.0125	13.962	13.468	13.057	12.723	12.460	12.237
	0.246	0.0700	0.0114	0.0200	14.214	13.685	13.269	12.928	12.641	12.392
	0.461	0.0688	0.0112	0.0369	14.565	14.039	13.594	13.242	12.970	12.758
	0.511	0.0686	0.0111	0.0407	14.761	14.225	13.781	13.425	13.146	12.924

Table 20
Enthalpy of activation for viscous flow ΔH^*/kJ·mol^{-1} and entropy activation for viscous flow ΔS^*/J·(mol·K)$^{-1}$.

AMP/MEA mass %	x_4	ΔH^*/kJ·mol^{-1}	ΔS^*/J·(mol·K)$^{-1}$
21/9	0.0000	22.733	32.622
	0.0095	22.598	31.278
	0.0185	22.764	31.219
	0.0269	22.958	30.918
	0.0346	23.328	31.484
	0.0444	23.331	30.796
24/6	0.0000	23.250	33.979
	0.0071	23.547	34.446
	0.0141	23.573	33.693
	0.0264	23.898	33.757
	0.0349	24.652	35.323
	0.0420	24.735	34.904
27/3	0.0000	24.152	36.711
	0.0059	23.699	34.513
	0.0125	24.030	34.717
	0.0200	24.772	36.412
	0.0369	25.152	36.537
	0.0407	25.492	37.032

Declaration of competing interest

The authors declare no competing financial interest.

Acknowledgement

This work was supported by the Ministry of Education and Research of the Norwegian Government.

Appendix A. Supplementary data

Supplementary materials include a comparison of measured viscosity with literature, pH variation in the CO_2 loaded aqueous amine mixtures and developed MATLAB programs for the density and viscosity data fittings. Supplementary data to this article can be found online at doi:https://doi.org/10.1016/j.molliq.2020.113286.

References

[1] P. Singh, D.W.F. Brilman, M.J. Groeneveld, Energy Procedia 1 (2009) 1257.
[2] S.K. Wai, C. Nwaoha, C. Saiwan, R. Idem, T. Supap, Sep. Purif. Technol. 194 (2018) 89.
[3] A. Hartono, H.F. Svendsen, J. Chem. Thermodynamics 41 (2009) 973.
[4] A. Dey, A. Aroonwilas, Energy Procedia 1 (2009) 211.
[5] R. Sakwattanapong, A. Aroonwilas, A. Veawab, Energy Procedia 1 (2009) 217.
[6] M. Usman, Department of Chemical Engineering, Norwegian University of Science and Technology, 2012.
[7] M.H. Li, B.C. Chang, J. Chem. Eng. Data 40 (1995) 328.
[8] M.H. Li, M.D. Lai, J. Chem. Eng. Data 40 (1995) 486.
[9] D. Śpiewak, A. Krótki, T. Spietz, M. Stec, L. Więcław–Solny, A. Tatarczuk, A. Wilk, Chem. Process. Eng. 36 (2015) 39.
[10] A. Aroonwilas, A. Veawab, Energy Procedia 1 (2009) 4315.
[11] G. Sartori, D.W. Savage, Ind. Eng. Chem. Fundamen. 22 (1983) 239.
[12] C. Nwaoha, C. Saiwan, T. Supap, R. Idem, P. Tontiwachwuthikul, W. Rongwong, M.J. Al-Marri, A. Benamor, Int. J. Greenhouse Gas Control 53 (2016) 292.
[13] B.P. Mandal, S.S. Bandyopadhyay, Chem. Eng. Sci. 61 (2006) 5440.
[14] B.P. Mandal, M. Kundu, S.S. Bandyopadhyay, J. Chem. Eng. Data 48 (2003) 703.
[15] M.-H. Li, Y.-C. Lie, J. Chem. Eng. Data 39 (1994) 444.
[16] O. Redlich, A.T. Kister, Ind. Eng. Chem. 40 (1948) 345.
[17] R.H. Weiland, J.C. Dingman, D.B. Cronin, G.J. Browning, J. Chem. Eng. Data 43 (1998) 378.
[18] H. Eyring, J. Chem. Phys. 4 (1936) 283.
[19] J. Han, J. Jin, D.A. Eimer, M.C. Melaaen, J. Chem. Eng. Data 57 (2012) 1095.
[20] S. Jayarathna, A. Weerasooriya, S. Dayarathna, D.A. Eimer, M.C. Melaaen, J. Chem. Eng. Data 58 (2013) 986.
[21] Z. Idris, N.B. Kummamuru, D.A. Eimer, J. Mol. Liq. 243 (2017) 638.
[22] JCGM 2008 (2008) JCGM 101.
[23] S.L.R. Ellison, A. Williams, 2012.
[24] J. Aguila-Hernández, R. Gómez-Quintana, F. Murrieta-Guevara, A. Romero-Martínez, A. Trejo, J. Chem. Eng. Data 46 (2001) 861.
[25] A. Henni, J.J. Hromek, P. Tontiwachwuthikul, A. Chakma, J. Chem. Eng. Data 48 (2003) 551.
[26] S. Xu, F.D. Otto, A.E. Mather, J. Chem. Eng. Data 36 (1991) 71.
[27] K. Zhang, B. Hawrylak, R. Palepu, P.R. Tremaine, J. Chem. Thermodyn. 34 (2002) 679.
[28] S. Paul, B. Mandal, J. Chem. Eng. Data 51 (2006) 1808.
[29] A.J. Treszczanowicz, G.C. Benson, J. Chem. Thermodyn. 10 (1978) 967.
[30] H. Iloukhani, M. Rezaei-Sameti, J. Basiri-Parsa, J. Chem. Thermodyn. 38 (2006) 975.
[31] A.A. Rostami, M.J. Chaichi, M. Sharifi, Monatshefte für Chemie - Chemical Monthly 138 (2007) 967.
[32] S.C. Bhatia, R. Bhatia, G.P. Dubey, J. Mol. Liq. 144 (2009) 163.
[33] A. Hartono, E.O. Mba, H.F. Svendsen, J. Chem. Eng. Data 59 (2014) 1808.
[34] S.A. Jayarathna, C.K. Jayarathna, D.A. Kottage, S. Dayarathna, D.A. Eimer, M.C. Melaaen, J. Chem. Eng. Data 58 (2013) 343.
[35] M. Shokouhi, A.H. Jalili, F. Samani, M. Hosseini-Jenab, Fluid Phase Equilib. 404 (2015) 96.
[36] J. Setschenow, Z. Phys. Chem. (1889) 117.
[37] J.M. Prausnitz, R.N. Lichtenthaler, E.G.d. Azevedo, Molecular thermodynamics of fluid-phase equilibria, Prentice Hall PTR, 1999.
[38] A.H. Harvey, Thermodynamic properties of water, NIST, Boulder, Colorado, 1998.
[39] T.G. Amundsen, L.E. Øi, D.A. Eimer, J. Chem. Eng. Data 54 (2009) 3096.
[40] E.N.d.C. Andrade, 17 (1934) 698.
[41] D.H. Vogel, Phys. Z. 22 (1921) 645.
[42] D. Fu, H. Hao, F. Liu, J. Mol. Liq. 188 (2013) 37.
[43] R.B. Bird, W.E. Stewart, E.N. Lightfoot, Transport Phenomena, second edition edn John Wiley & Sons, Inc, USA, 2002.
[44] R. Meyer, M. Meyer, J. Metzger, A. Peneloux, Journal de Chimie Physique et de Physico-Chimie Biologique 68 (1971) 406.
[45] C.M. Kinart, W.J. Kinart, A. Ćwiklińska, J. Therm. Anal. Calorim. 68 (2002) 307.
[46] S. Oswal, M.V. Rathnam, Can. J. Chem. 62 (1984) 2851.
[47] A. Ćwiklińska, C.M. Kinart, J. Chem. Thermodyn. 43 (2011) 420.
[48] T.M. Aminabhavi, M.I. Aralaguppi, G. Bindu, R.S. Khinnavar, J. Chem. Eng. Data 39 (1994) 522.
[49] K. Ohnishi, I. Fujihara, S. Murakami, Fluid Phase Equilib. 46 (1989) 73.
[50] N.S. Matin, J.E. Remias, K. Liu, Ind. Eng. Chem. Res. 52 (2013) 16979.